Original Paper

Effects of water immersion on shear bond strength reduction after current application of resin-modified glass-ionomer-cements with and without an ionic liquid

Hiroko SATO[1], Yuta MATSUKI[1], Noboru KAJIMOTO[2*], Emi UYAMA[2], Shinya HORIUCHI[1], Kazumitsu SEKINE[2], Eiji TANAKA[1], and Kenichi HAMADA[2]

[1]Department of Orthodontics and Dentofacial Orthopedics, Institute of Biomedical Sciences, Tokushima University Graduate School, 3-18-15 Kuramoto, Tokushima 770-8504, Japan

[2]Department of Biomaterials and Bioengineering, Institute of Biomedical Sciences, Tokushima University Graduate School, 3-18-15 Kuramoto, Tokushima 770-8504, Japan

[*]present affiliation: Section of Bioengineering, Department of Dental Engineering, Fukuoka Dental College, Fukuoka 814-0193, Japan

Key words: Glass-ionomer-cement, Shear bonding strength, Ionic-liquid, Electric conductivity, Smart adhesive

Number of reprints: 0

Corresponding author: Kenichi HAMADA; hamada.dent@tokushima-u.ac.jp, Tel: 088-633-7334, Fax: 088-633-9125

ABSTRACT

The enhancement in the bonding strength of advanced dental cements has enabled long-lasting dental restorations. However, the high bonding strength can cause difficulty in removing these restorations. Therefore, “smart” dental cements with simultaneous strong bonding and easy on-demand debonding ability are required. A resin-modified glass-ionomer-cement (RMGIC) with an ionic liquid (IL) has demonstrated significant reduction in the bonding strength with current application (CA). This research investigates the effects of immersion in distilled water on the electric conductivity and bonding strength of RMGIC with and without an IL and CA. The RMGIC without the IL exhibited significant electric conductivity after immersion, and a significant decrease in bonding strength with CA. In comparison, the electric conductivity after immersion and the decrease in bonding strength with CA were greater for RMGIC with the IL. Thus, the feasibility of smart dental cements capable of electrically debonding-on-demand is indicated.

INTRODUCTION

New and advanced dental cements exhibit superior properties compared to those of conventional materials[1]; especially, the improvement in the bonding strength gives patients the assurance of a better durability of their dental devices. However, the high bonding strength occasionally causes difficulties in the removal of the devices, which is needed in several circumstances: the removal of restorations is necessary for treating the patient from the incidence of secondary caries; removal of orthodontic brackets is required after the completion of an orthodontic treatment; and the removal of dental implant abutments is appropriate for the periodical maintenance of cement-retained dental implants. Furthermore, excessive force or vibrations is required for the removal of these devices, which occasionally leads to damages to the enamel, dentin, and teeth roots. Hence, the use of a "smart" dental cement exhibiting an adjustable bonding strength which is controllable on-demand is required in order to simultaneously have strong bonding and easy debonding.

Adhesives for engineering applications exhibiting easy on-demand debonding have been developed and released[2]. In contrast, the development of such adhesives for dental applications has only just started and has only been reported recently[3-7]. Many of these adhesives use heat as a trigger to reduce the bonding strength, taking advantage of softening, melting, or bubbling of the adhesives at high temperatures[8]. However, heating of adhesives in the oral cavity has the potential risk of damaging to the oral mucosa. Thus, an electric current

has been adopted as the trigger in this work. We have developed a prototype Resin-Modified Glass-Ionomer-Cement (RMGIC) with a ionic-liquid (IL), and validated the concept of a "dental cement debonding on-demand in response to an electric current trigger" in a previous paper[9].

One of the important properties of RMGICs today is the ability to release fluoride ions and other biologically active ions in the oral cavity[10]. This property suggests that IL contained in the prototype cement can also be released in the oral cavity, which leads to a reduction in the electric conductivity of the cement and the loss of this on-demand controllable debonding ability. However, only prototype cements stored in air were evaluated in the previous study. Therefore, evaluation of these materials stored in liquids (e.g. saliva, water, and different kinds of drinks), is required to validate the effectiveness of the smart dental cement in the oral cavity. In this paper, our prototype RMGIC with an IL was stored in distilled water and monitored over time, and the changes in its electrical properties and bonding properties were evaluated. A RMGIC without an IL was also stored under the same conditions and evaluated as a control.

MATERIALS AND METHODS

Prototype cement preparation

The IL used in this study was tris(2-hydroxyethyl)methylammonium methylsulfate (Sigma-Aldrich Japan K.K., Tokyo, Japan), the same one employed in the previous study[9]. It was considered suitable for the preparation of prototype cements due to its low toxicity and the

absence of skin irritation. A commercial RMGIC (RelyX^{TM} Luting Plus, 3M Japan Limited, Tokyo, Japan) was utilized as the base cement. The composition of the RMGIC is presented in Table 1. The IL mixing ratios (wt.%) were 0% (RX0) and 10% (RX10). The IL and two cement pastes (a base paste and a catalyst paste) were mixed simultaneously using a plastic sterile spatula on a mixing paper.

Specimen preparation for the evaluation of the shear bond strength

Dental cements are mainly utilized for the bonding of restorative materials to the dentin or the enamel. Thus, the bonding strength between these restorative materials and the dentin/enamel should be evaluated for perspective clinical applications. However, in this study, only the bonding strength between two metals was evaluated, because the objective was to clarify the effects of water immersion on the electrical properties and bonding properties of the prototype cement and to validate bonding strength reduction upon current application (CA). In our previous study[9)], Cu was adopted as the adherend material because of its high electric conductivity. In contrast, Ti was adopted in this study because the corrosion resistance of Cu in water is inadequate.

Two Ti rods (Ø8 mm×10 mm and Ø20 mm×10 mm (diameter×length)) were used to assemble the specimens. The cross section of the rods was sanded using 600 grit SiC waterproof paper, and then the circular bonding area of both rods was roughened by sandblasting (alumina particles of 50 μm diameter, sandblasting pressure of 0.4 MPa). After uniformity of the surface

roughness was verified visually, the rods were rinsed ultrasonically in distilled water for 5 min. The cement was then spread on the cross section of the Ø8 mm Ti rod, and it was set at the center of the Ø20 mm Ti rod. The pair of rods were pressed at a pressure of 20 g/mm^2 for 5 min and the excess cement was removed manually. 30 min after bonding, the specimens subject to water immersion were left into distilled water and then kept either for 1 day, 7 days, or 14 days, and the specimens not subject to water immersion were stored in air for 24 hours (immersion for 0 day). Distilled water (100 mL for one sample, 37°C) was exchanged every 3.5 days.

Current application to the specimens

Direct currents of 19 V were applied for 30 s on the specimens in air using a programmable power supply (Type 7651, Yokogawa Electric Corp., Tokyo, Japan). These conditions were set to be equal to those for the removal of ElectRelease$^{TM11)}$. The Ø20 mm rod was set as the anode. The changes in current with time were recorded using a digital multimeter (Type TY720, Yokogawa Electric Corp., Tokyo, Japan), and the total charge density applied on the specimens was calculated from the time-integrated current values.

Bonding strength evaluation

A universal testing machine (AGS-500A, Shimadzu Corp., Kyoto, Japan) was utilized for the evaluation of the shear bond strength, σ_s. The specimen setting in the compression test jig is schematically shown in Fig. 1. The cross head speed was set to 0.5 mm/min. σ_s was calculated

as follows:

$$\sigma_s = L/S \quad (1)$$

where σ_s is the shear bond strength, L is the load at fracture, and S is the bonding area (50.24 mm^2 in this study). To clarify the effects of CA on σ_s values, the specimens were evaluated with and without CA.

The total specimen preparation and σ_s evaluation flow is summarized in Fig. 2, and the number of the specimens of each group are indicated in Fig. 2.

Fracture surface observation

After σ_s evaluation, the fracture surfaces of the specimens were photographed using digital cameras with automatic white-balance and exposure settings.

Statistical evaluation

The data for σ_s was statistically analyzed using the Steel-Dwass Test performed by the EZR software (Saitama Medical Center, Jichi Medical University, Japan)[12] to compare the mean values from different groups. Statistical significance was accepted at a confidence level of 0.05 or 0.01.

The σ_s measurements data was also investigated using a two-parameter Weibull distribution analysis (Eq. 2) applying the Bemard's median rank method (Eq. 3)[13, 14].

$$P = 1 - \exp\left[-\left(\frac{\sigma_S}{\sigma_0}\right)^m\right] \quad (2)$$

$$P = \frac{i-0.3}{n+0.4} \quad (3)$$

Where P is the cumulative probability of fracture, σ_s is the shear bond strength, σ_0 is the scale parameter, m is the Weibull modulus (shape parameter), i indicates that a σ_s value ranks the ith in the ascending order of magnitude for σ_s and n is the number of total data point. Linear regression analysis was carried out to Weibull plots of $\ln[\ln(1/1-P)]$ vs. $\ln(\sigma_s)$, then, the Weibull modulus and scale parameter have been estimated.

RESULTS

Charge density

Fig. 3 shows the effect of the duration of immersion in distilled water on charge density with CA, and Table 2 shows the statistical analysis of these results. The charge density average for the RX0 specimens subject to water immersion was significantly higher than that of the specimens not subjected to water immersion, however, there was no significant effect of the immersion period on charge density. Although the immersion time did not have a significant effect on the charge density, the trend of the average values for multiple samples potentially shows reduction and saturation with increasing immersion time from 1 day to 14 days. In contrast, the charge densities of the RX10 specimens with and without water immersion did not show a significant difference.

Although there was no significant influence of the immersion period, the average value potentially shows a higher value after the first day, which decreased and eventually reached a plateau with increased immersion time from 1 day to 14 days. A comparison of the results from the RX0 specimens and the RX10 specimens indicates that the RX10 specimens not exposed to water and those subject to 7 days and 14 days of immersions showed a significantly higher charge density average compared to those of the RX0 specimens.

Shear bond strength

Fig. 4 shows the effect of immersion time on σ_s, and Table 3 shows the statistical analysis of these findings. The immersion time did not have a significant effect on σ_s for both the RX0 specimens and the RX10 specimens without CA. In contrast, σ_s of the RX0 specimens and the RX10 specimens after 1 day immersion with CA showed a significant decrease compared to the case where the specimens were not immersed. In particular, for the RX10 specimens after 1 day immersion and CA, the σ_s reached the lowest value in this study. The σ_s of the RX0 specimens and the RX10 specimens with CA increased significantly with immersion from day 1 to day 7. The average value of the RX10 specimens with CA showed an initial increase and subsequent saturation with increasing immersion time from 1 day to 14 days, and that of the RX0 specimens showed a similar trend. Comparison of σ_s values with and without CA indicates that for RX10 specimens, the average σ_s with CA was significantly lower than that without CA;

however, for the RX0 specimens with CA subject to 7 days and 14 days immersion, σ_s did not show a significant decrease compared to those without CA. Besides, without CA, σ_s of the RX10 specimens was significantly lower than that of the RX0 specimens, and also with CA, σ_s of the RX10 specimens was significantly lower than that of the RX0 specimens ($p<0.01$, not indicated in Table 3).

Figs. 5 and 6 show the Weibull plots of σ_s of the RX0 specimens with and without CA, and that of the RX10 specimens with and without CA, respectively. The Weibull modulus and scale parameter estimated are shown in Table 3. The Weibull modulus of the RX0 specimens without CA had the highest value in this study. Both the RX0 and RX10 specimens with 1 day immersion with CA exhibited the smallest Weibull modulus. Note that the RX10 specimens subject to 1 day immersion with CA showed an extremely small Weibull modulus and the Weibull plot showed a non-linear trend.

Effect of charge density on the shear bond strength

Fig. 7 shows the effect of charge density on the σ_s for the RX0 specimens and the RX10 specimens. As seen, σ_s decreased linearly with increasing charge density from 0 to ~1 mC/mm^2.

Fracture surface after the shear bond strength test

Fig. 8 shows the typical fracture surfaces of Ti rods of the RX0 specimens and the RX10

specimens after 1 day of immersion with and without CA, after they were subjected to the shear bond strength test. Both the Ti surface and cement residues were observed without CA on the surface of many specimens, which indicates that the fracture was mixed mode; however, few specimens showed interface fracture. In contrast, no cement residue was observed on the anode of many specimens with CA, indicating that the fracture was interfacial at the anode. However, few RX0 specimens showed mixed mode fracture. Correlation between the shear bonding strength and fracture mode was not clear in this research.

DISCUSSION

Changes in charge density with increasing immersion period

The base RMGIC for the prototype cement before curing contains water-soluble polymers and polymerizable monomers, glass fillers, tartaric acid, and water[15]. Thus, the base RMGIC can exhibit electric conductivity in case if tartaric acid is not consumed completely in the acid-base reaction occurring during the curing phase and if water is not completely consumed or released from the cement. Fig. 3 indicates that the RX0 specimens without immersion showed only small charge density values, and the RX0 specimens after 1 day immersion showed a significant increase in charge density. This fact suggests that our RMGIC is not an electrical insulator but a weak electrical conductor, and that it can increase its electric conductivity with water absorption. The charge density average value for the RX0 specimens decreased with increased immersion period from day 1 to day 7. The difference was not significant; however, the average

value showed a decreasing trend from 1 day to 7 days of immersion, and then saturated at a higher value than those of the same samples without immersion. This decrease was potentially caused by a release of tartaric acid from the specimen. Therefore, we would expect that the charge density keeps decreasing with increased immersion period. To verify that the charge density decrease really plateaus, an evaluation of the effect of a longer immersion time for the RX0 specimens is required.

With the IL, the RX10 specimens showed a significantly higher charge density average than did the RX0 specimens, indicating that IL addition is effective to increase the electric conductivity of an RMGIC. Although the difference was not significant, the charge density value increased after 1 day of immersion and then decreased over 7 days and 14 days. The dependence of charge density for the RX10 specimens on immersion time was similar to that of the RX0 specimens. The increase was also caused by water absorption, while the decrease was also caused by a release of tartaric acid and/or IL from the specimen. The increment in the charge density value from 0 day immersion to 1 day immersion of the RX10 specimens was smaller than that of the RX0 specimens, but the reason for this was not clarified in this study. Note that the charge density values of the RX10 specimens with immersion periods longer than 7 days were nearly equal to those of the samples without immersion, demonstrating that the RX10 specimens hardly loses any electric conductivity solely because of the effect of distilled water.

Changes in shear bond strength after current application and with increasing immersion periods

Fig. 4 shows that the decrease of σ_s for the RX0 specimens due to CA was not necessarily significant, however the average value decreased slightly due to CA, regardless. The decrease of σ_s for the RX0 specimens after 1 day immersion due to CA was the largest, which is comparable to the large charge density change in the RX0 specimens after 1 day of immersion. Note that the RMGICs without IL possibly show an on-demand debonding property with CA, based on their electric conductivity. This finding reminds us that an applied Galvanic current potentially has the risk of reducing the bonding strength between metal restorations and dentin in the oral cavity, resulting a premature and uncontrolled debonding of the restorations. However, the decrease of σ_s for the RX0 specimens shows a decrease with increasing immersion period, promising an alleviation of the risk over time after bonding. Fig. 7 shows that the average σ_s for the RX0 monotonously decreased with increasing charge density. This dependence was similar to that in our previous study[9], however, average σ_s for the RX0 samples showed a linear decrease in these experiments, while it showed an exponential decrease in the previous study. The reason of this mismatch was not yet clarified. One possible reason is that the bonding metal in this study was titanium, while copper was used in the previous experiments. A linear and monotonous decrease of σ_s was also observed for the RX10 specimens, and the

dependence of the σ_s on charge density was also similar to the other specimens.

Fig. 4 shows that σ_s for the RX10 specimens not subject to immersion without CA was significantly lower than that of the RX0 specimens without CA, indicating that 10% IL in the material was excessive and reduced σ_s. We have evaluated specimens with low IL and found σ_s to increase with decreasing IL content, and on the other hand, electric conductivity decreased with decreasing IL content. Since the decrease in electric conductivity requires longer periods to perform on-demand debonding[9)], optimization of the IL content to achieve both optimal initial σ_s and appropriate periods to perform on-demand debonding required.

Such as the decrease of σ_s in the RX0 specimens, the decrease of σ_s value for the RX10 specimens after 1 day immersion due to CA was very substantial, which is compatible with the large difference in charge density in the RX10 specimens in the same conditions. The change in σ_s for the RX10 specimens with CA was found to be larger than that of the RX0 specimens subject to the same immersion periods in this study, which is also compatible with the results that a larger change in charge density value is observed for the RX10 specimens compared to the RX0 specimens. This result indicates that IL addition to RMGICs is effective to reduce the σ_s with CA. The decrease of σ_s slowed down from 1 day immersion to 7 days immersion and 14 days immersion; however, the decrease was completely saturated after 7 days of immersion. This fact suggests that the imperfect permanence of ion content in distilled water decreases the electric conductivity of the prototype cement and sequentially inhibits the reduction of σ_s with

CA, but this inhibition effect will not be rapid.

Weibull plots of σ_s values shown in Figs. 5 and 6 did not reveal remarkable differences between different cases, except for σ_s values of the RX0 specimens with 1 day of immersion with CA. The RX0 specimens not subject to immersion without CA demonstrated the largest Weibull modulus, namely, the σ_s value distribution for the RX0 specimens without immersion and without CA was the smallest. The property of the other specimens changed due to a manual mixing of the IL into the RMGIC and subsequent immersion in distilled water, as well as CA. These alterations potentially enlarged the distribution of σ_s values; in particular, manually obtaining a homogeneous mixture of IL and RMGIC was difficult because of the high viscosity of the IL chosen. Note that the Weibull plot for the σ_s values of the RX0 specimens with CA after 1 day of immersion was apparently different from those of the other plots; it did not show a linear trend and potentially showed a minimum σ_s value at approximately 0.1 MPa. These results suggest that a truncated Weibull distribution analysis (Eq. 4) is more appropriate in this situation[16].

$$P = 1 - \exp\left[-\left(\frac{{\sigma_S}^m - t^m}{{\sigma_0}^m}\right)\right] \quad (4)$$

Where P, σ_s and σ_0 are the same as those in Eq. 2, and t is the truncation limit. The truncation limit of σ_s indicates the minimum σ_s value at which the specimen was found to be durable to the shear bonding strength test in our experiments. Under the truncation limit, the bonding in the specimen was damaged, and debonding happened during the experimental procedure of

current application, or while setting the sample in the test apparatus. Thus, the data acquisition of very low σ_s values was impossible, and these data was ignored in the two-parameter Weibull distribution analysis. Fig. 9 shows the truncated Weibull distribution analysis with a scale parameter of 0.01 MPa, a Weibull modulus (shape parameter) of 0.33, and a truncated limit of 0.08 MPa. We can see that it shows a more accurate representation of the behavior of the RX10 specimens with 1 day immersion with CA. This consideration suggests that two-parameter Weibull analysis of the entire data set, including lower σ_s value data not acquired in this research, will indicate smaller scale parameters and smaller Weibull parameters. Conversely, the two-parameter Weibull analysis result overestimate the value of σ_s and underestimate the distribution of σ_s values for the RX10 specimens with 1 day immersion with CA.

Effects of current application on the bonding between the cement and titanium

Fig. 8 shows that an interface fracture with CA was observed only on the anode. This result coincides with the fracture pattern obtained in the previous study[9]. Therefore, the reason for the decrease of σ_s was possibly similar: Ti ions release, and/or a potential Ti compounds formation damages the interfacial bonding between the cement and the anode. Thus, a large charge density should promote reduction in σ_s.

Future work

It is widely recognized that many RMGIC-based products today show not only the release of fluoride ions, but also their recharge[17-19]. This phenomenon suggests that RMGICs potentially absorb the ions contained in the oral cavity, e.g. saliva, drinks and foods containing salts, resulting in a maintenance of a somewhat high electric conductivity for long periods. Thus, in our next investigation, the prototype cement explored in this research will be immersed in saline or artificial saliva, and the changes in charge density and decrease in bonding strength with CA will be evaluated.

CONCLUSION

Resin-modified glass-ionomer-cements with or without ionic liquids were produced and immersed in distilled water over different time scales, and their properties were evaluated. The following conclusions can be drawn:

1. RMGICs without ILs exhibited significant electric conductivity after immersion, and a significant bonding strength decrease after current application.
2. RMGICs with ILs exhibited larger electric conductivity than RMGICs without ILs after immersion, and more significant bonding strength decrease after current application.
3. The electric conductivity of RMGICs both with and without ILs increased after 1 day of immersion, and then decreased after 7 days and 14 days immersions. However, the values for samples tested after 14 days immersion were similar to, or larger, than those before

immersion.

4. The bonding strengths of the RMGICs with ILs after current application exhibited significant decreases after 14 days immersion, and eventually reached a plateau.

These results suggest that resin-modified glass-ionomer-cements with ionic liquids are potential "smart" dental cements and are not subject to substantial impairment of their properties after immersion in the liquids of the oral cavity.

ACKNOWLEDGMENTS

This study was partially supported by JSPS KAKENHI Grant Numbers JP19K10184, 19K19054, 18K09855, 16K15804. The authors would like to express their gratitude to 3M Japan Limited for supplying the materials used in this study.

REFERENCES

1) Yu H, Zheng M, Chen R, Cheng H. Proper selection of contemporary dental cements. Oral Health Dent Manag 2014; 13: 54-9.
2) Lu Y, Broughton J, Winfield P. A review of innovations in disbonding techniques for repair and recycling of automotive vehicles. Int J Adhes Adhes 2014; 50: 119-27.
3) Tsuruoka T, Namura Y, Shimizu N. Development of an easy-debonding orthodontic adhesive using thermal heating. Dent Mater J 2007; 26: 78-83.
4) Ryu C, Namura Y, Tsuruoka T, Hama T, Kaji K, Shimizu N. The use of easily debondable orthodontic adhesives with ceramic brackets. Dent Mater J 2011; 30: 642-7.
5) Saito A, Namura Y, Isokawa K, Shimizu N. CO 2 laser debonding of a ceramic bracket bonded with orthodontic adhesive containing thermal expansion microcapsules. Lasers Med Sci 2015; 30: 869-74.
6) Bishti S, Tuna T, Agrawal G, Pich A, Wolfart S. Modified Glass Ionomer Cement with "Remove on Demand" Properties: An In Vitro Study. Dent J 2017; 5: 9.
7) Schenzel AM. Advanced Debonding on Demand Systems for Dental Adhesives: Karlsruher Institut für Technologie; 2017.
8) Luo X, Lauber KE, Mather PT. A thermally responsive, rigid, and reversible adhesive. Polym 2010; 51: 1169-75.
9) Kajimoto N, Uyama E, Sekine K, Hamada K. Electrical shear bonding strength reduction of resin-modified glass-ionomercement containing ionic-liquid: Concept and validation of a smart dental cement debonding-on-demand. Dent Mater J 2018; 37: 768-74.
10) Sidhu SK, Nicholson JW. A review of glass-ionomer cements for clinical dentistry. J Funct Biomater 2016; 7: 16.
11) Haydon D. ElectRelease–electrically disbonding epoxy adhesive. Assembly Autom 2002; 22: 326-9.
12) Kanda Y. Investigation of the freely available easy-to-use software 'EZR' for medical statistics. Bone Marrow Transpl 2013; 48: 452-8.
13) Xie L, Huang X, Li B-W, Zhi C, Tanaka T, Jiang P. Core–satellite Ag@BaTiO 3 nanoassemblies for fabrication of polymer nanocomposites with high discharged energy density, high breakdown strength and low dielectric loss. Phys Chem Chem Phys 2013; 15: 17560-9.
14) Singh S, Singh M, Prakash C, Gupta MK, Mia M, Singh R. Optimization and reliability analysis to improve surface quality and mechanical characteristics of heat-treated fused filament fabricated parts. Int JAdv Manuf Tech 2019; 102: 1521-36.
15) O'Brien WJ. Dental materials and their selection. Hanover Park: Quintessence; 2002.
16) Islam F, Joannès S, Bucknell S, Leray Y, Bunsell A, *et al*., Towards accurate and efficient

single fibre characterization to better assess failure strength distribution. ECCM 18 - 18th European Conference on Composite Materials, Jun 2018, Athens, Greece, 7 p.

17) Gao W, Smales R. Fluoride release/uptake of conventional and resin-modified glass ionomers, and compomers. J Dent 2001; 29: 301-6.

18) Gandolfi M, Chersoni S, Acquaviva G, Piana G, Prati C, Mongiorgi R. Fluoride release and absorption at different pH from glass-ionomer cements. Dent Mater 2006; 22: 441-9.

19) Mitra SB, Oxman JD, Falsafi A, Ton TT. Fluoride release and recharge behavior of a nano-filled resin-modified glass ionomer compared with that of other fluoride releasing materials. Am J Dent 2011; 24: 372.

Table and Figure captions

Table 1 Composition of the RMGIC utilized in this study (data obtained from manufacturer safety data sheets).

Table 2 Statistical analysis of the charge density with CA.

Table 3 Statistical analysis and Weibull parameter of the shear bonding strength with and without CA.

Fig. 1 Schematic drawing of (A) setting of electric current application to specimen, and (B) shear bonding strength test set-up.

Fig. 2 Specimen preparation and evaluation flow, and the number of specimens evaluated in this study.

Fig. 3 Effect of immersion period in distilled water on the charge density with CA.

Fig. 4 Effect of immersion period in distilled water on the shear bonding strength with and without CA.

Fig. 5 Weibull plot of the shear bonding strength of RX0 specimen with and without CA. The legends indicate immersion period in distilled water.

Fig. 6 Weibull plot of the shear bonding strength of RX10 specimen with and without CA. The legends indicate immersion period in distilled water.

Fig. 7 Correlation between the charge density and the shear bonding strength.

Fig. 8 Photographs and their schematic images of fracture surfaces on the RX0 specimen and RX10 specimen with 1 d immersion with and without CA after the shear bonding

strength test. Black area in the schematic images indicates the cement residue.

Fig. 9 Truncated Weibull analysis of the shear bonding strength of RX10 specimen with 1 d immersion with CA.

Table 1

Paste A	
Ingredient	mass%
Silane treated glass	70 - 80
Water	10 - 20
2-hydroxyethyl methacrylate (HEMA)	< 10
Silane treated silica	< 2
4-(dimethyamino)-benzeneethanol	< 1
Titanium dioxide	< 0.5

Paste B	
Ingredient	mass%
Silane treated ceramic	30 - 40
2-hydroxyethyl methacrylate (HEMA)	10 - 30
Copolymer of acrylic and itaconic acids	10 - 30
Water	5 - 15
Glycerol 1,3 dimethacrylate	1 - 5
Potassium diphosphate	1 - 5
Potassium persulfate	1 - 5
2,6-di-tert-butyl-p-cresol (BHT)	< 0.5
Ethylene dimethacrylate (EGDMA)	< 0.5

Table 2

specimen	immersion period in distilled water (day)	Significance (◆—◆ p<0.05) (●—● p<0.01)
RX0	0	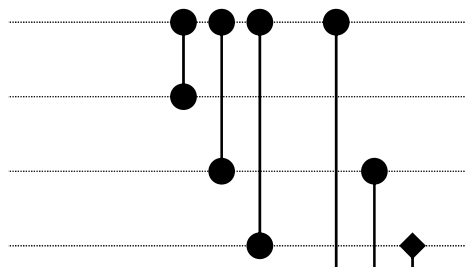
	1	
	7	
	14	
RX10	0	
	1	
	7	
	14	

Table 3

specimen	immersion period in distilled water (day)	significance (◆—◆ p<0.05) (●—● p<0.01)	Weibull modulus, m	scale parameter, σ_0
RX0 (without CA)	0	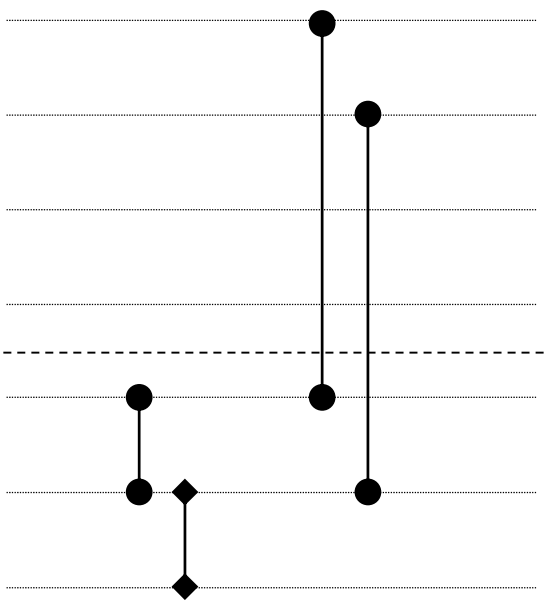	14.2	22.2
	1		6.3	19.7
	7		5.1	23.4
	14		6.3	19.6
RX0 (with CA)	0		7.5	17.4
	1		4.0	11.9
	7		10.4	16.8
	14		7.9	15.8
RX10 (without CA)	0	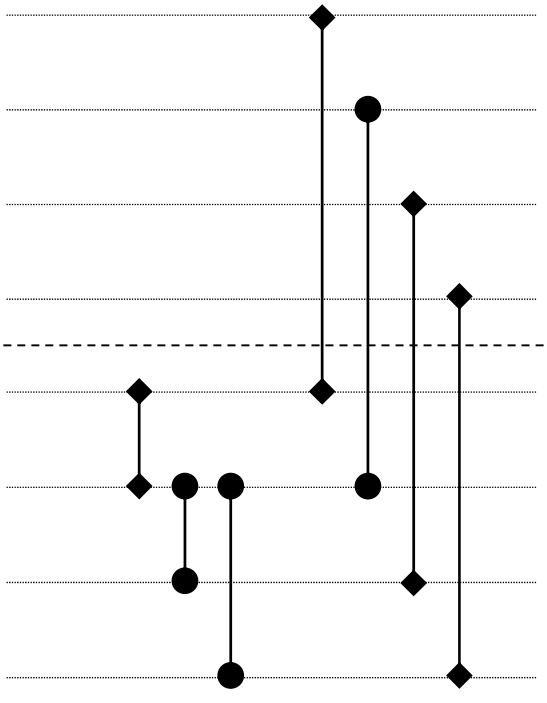	8.5	12.3
	1		11.0	10.9
	7		6.0	12.6
	14		6.9	10.8
RX10 (with CA)	0		4.6	4.5
	1		0.9	0.5
	7		4.7	5.5
	14		9.0	4.9

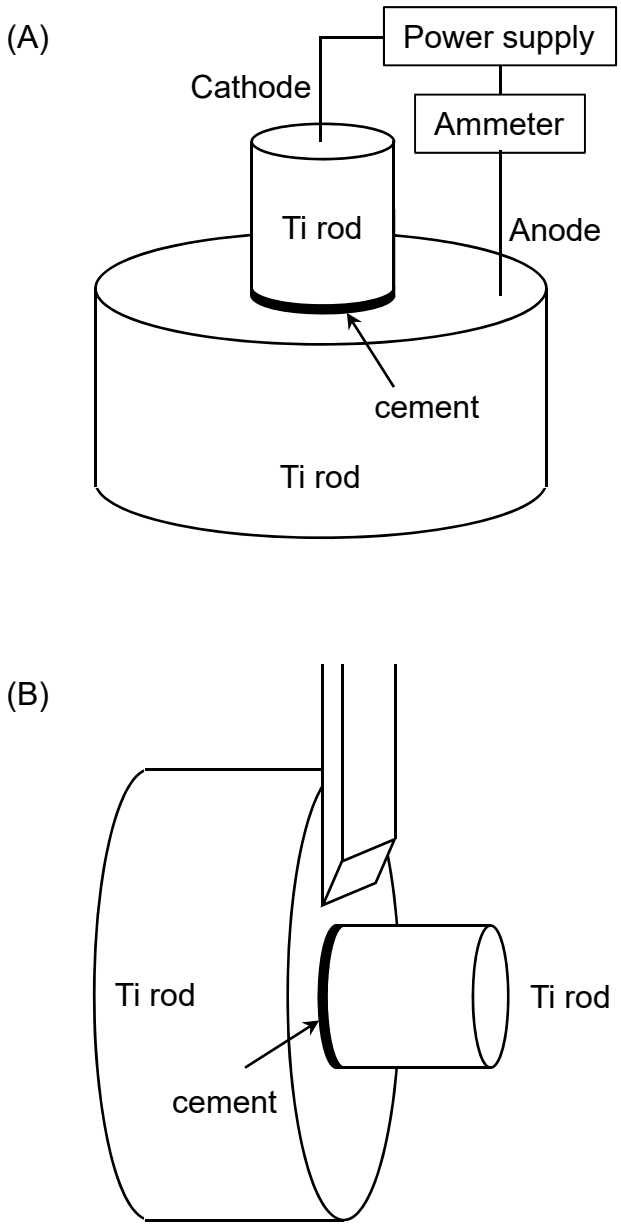
(A)
Power supply
Cathode
Ammeter
Ti rod
Anode
cement
Ti rod
(B)
Ti rod
Ti rod
cement

Fig. 1 (100%)

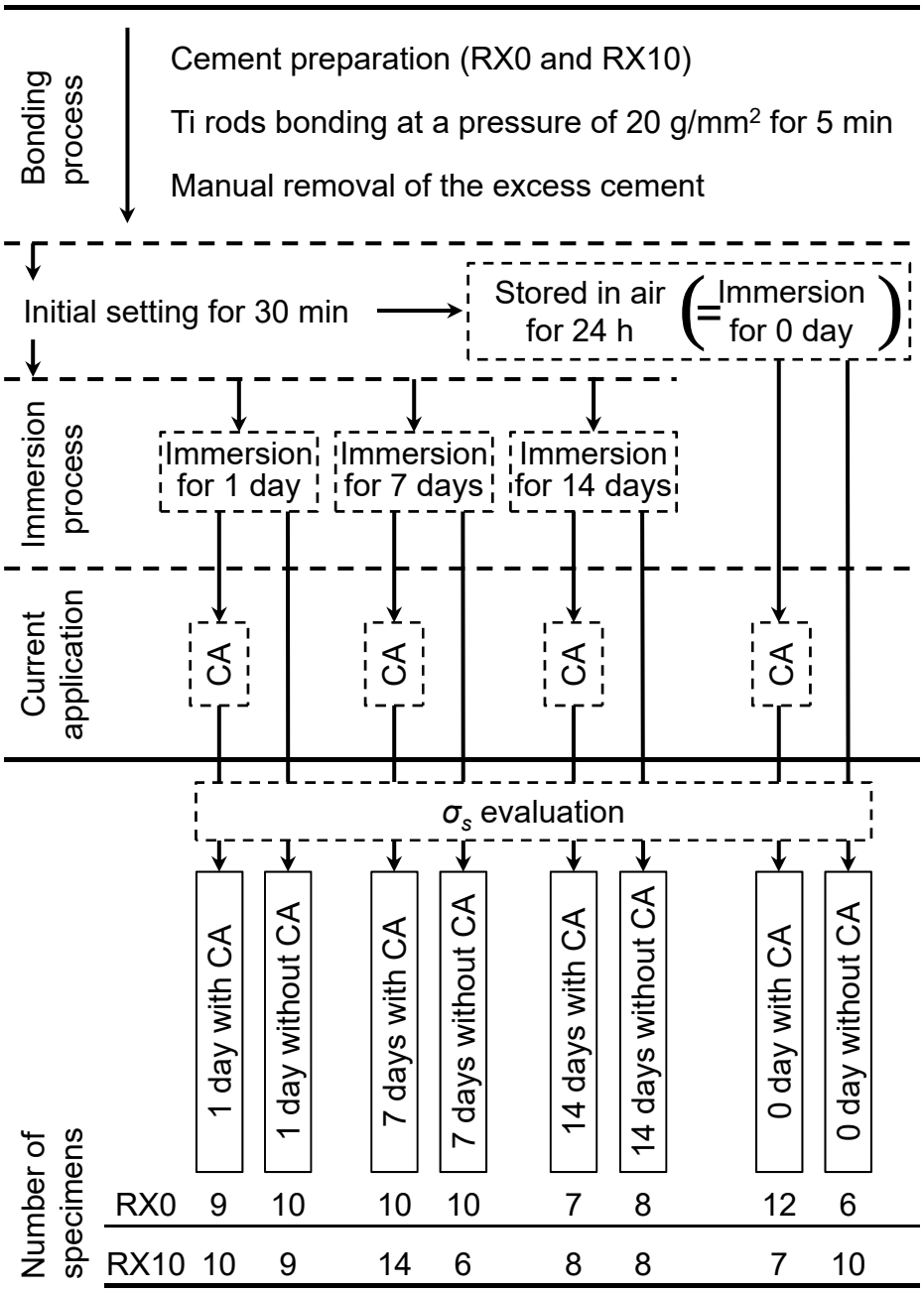
Bonding process
Cement preparation (RX0 and RX10)
Ti rods bonding at a pressure of 20 g/mm2 for 5 min
Manual removal of the excess cement
Initial setting for 30 min
Stored in air for 24 h
(=Immersion for 0 day)
Immersion process
Immersion for 1 day
Immersion for 7 days
Immersion for 14 days
Current application
CA
CA
CA
CA
σs evaluation
1 day with CA
1 day without CA
7 days with CA
7 days without CA
14 days with CA
14 days without CA
0 day with CA
0 day without CA
Number of specimens
RX0 9 10 10 10 7 8 12 6
RX10 10 9 14 6 8 8 7 10

Fig. 2 (100%)

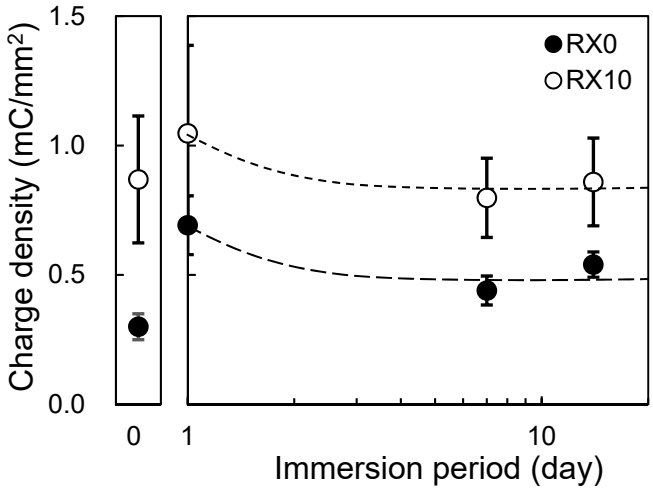
Charge density (mC/mm²)
1.5
1.0
0.5
0.0
RX0
RX10
0
1
10
Immersion period (day)

Fig. 3 (100%)

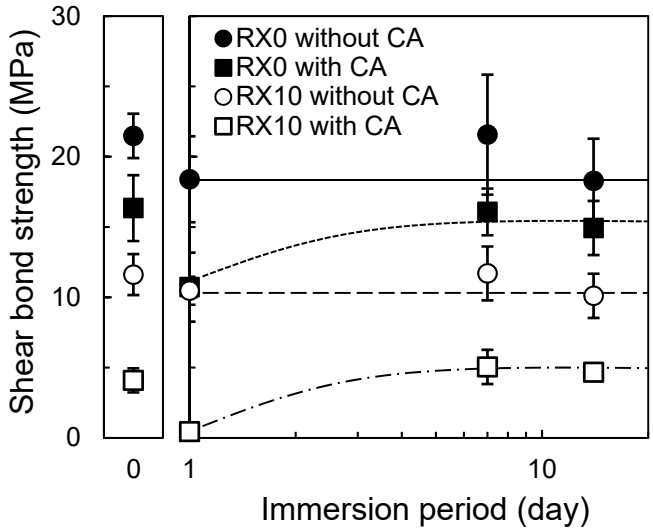
RX0 without CA
RX0 with CA
RX10 without CA
RX10 with CA
Shear bond strength (MPa)
30
20
10
0
0
1
10
Immersion period (day)

Fig. 4 (100%)

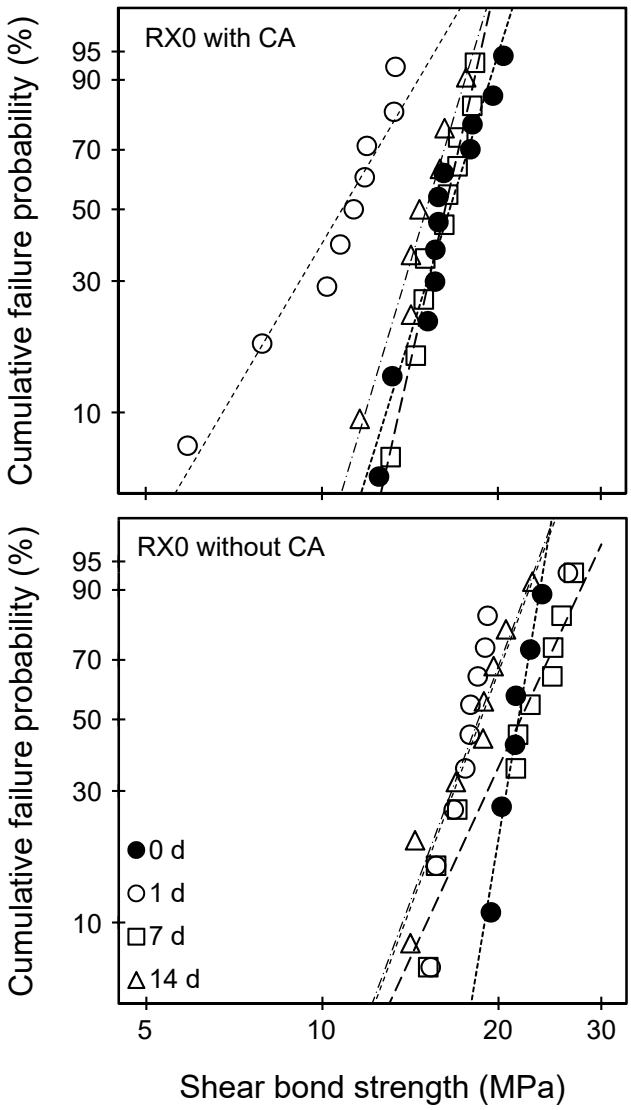
RX0 with CA
RX0 without CA
Cumulative failure probability (%)
95
90
70
50
30
10
0 d
1 d
7 d
14 d
5
10
20
30
Shear bond strength (MPa)

Fig. 5 (100%)

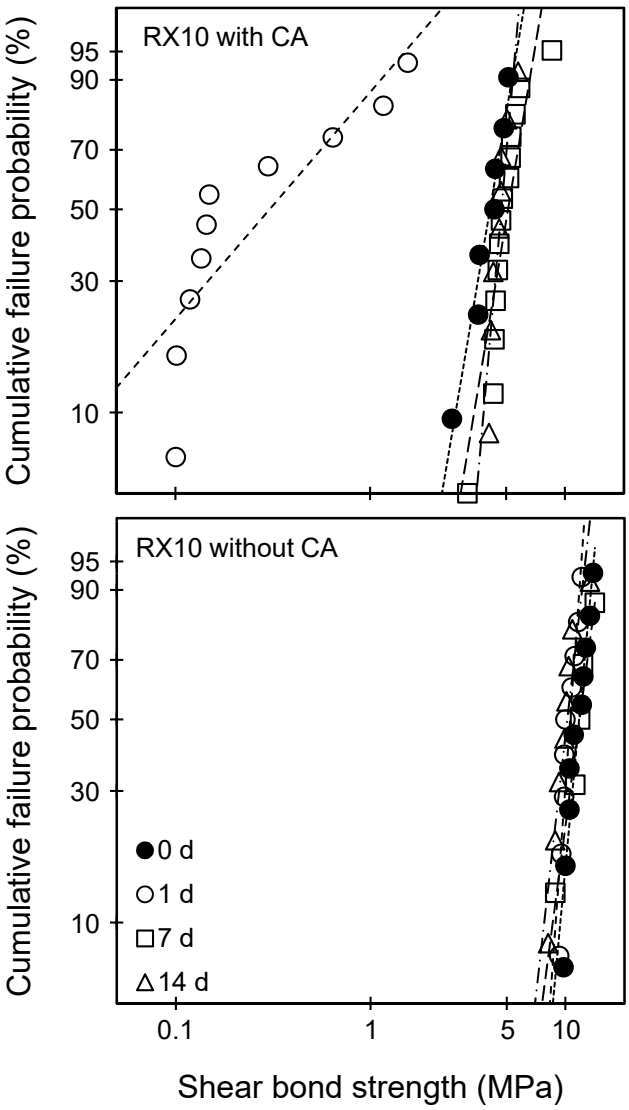
RX10 with CA
RX10 without CA
Cumulative failure probability (%)
95
90
70
50
30
10
0 d
1 d
7 d
14 d
0.1
1
5
10
Shear bond strength (MPa)

Fig. 6 (100%)

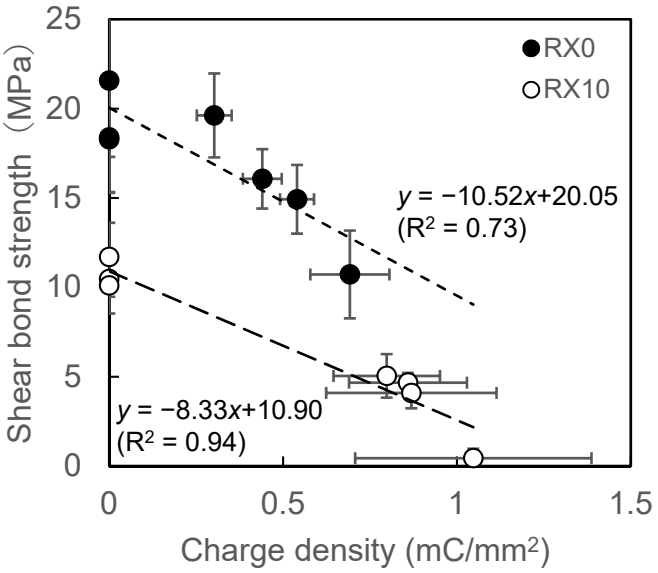
25
20
15
10
5
0
0
0.5
1
1.5
Shear bond strength（MPa）
Charge density (mC/mm2)
RX0
RX10
y = −10.52x+20.05
(R2 = 0.73)
y = −8.33x+10.90
(R2 = 0.94)

Fig. 7 (100%)

Camera images

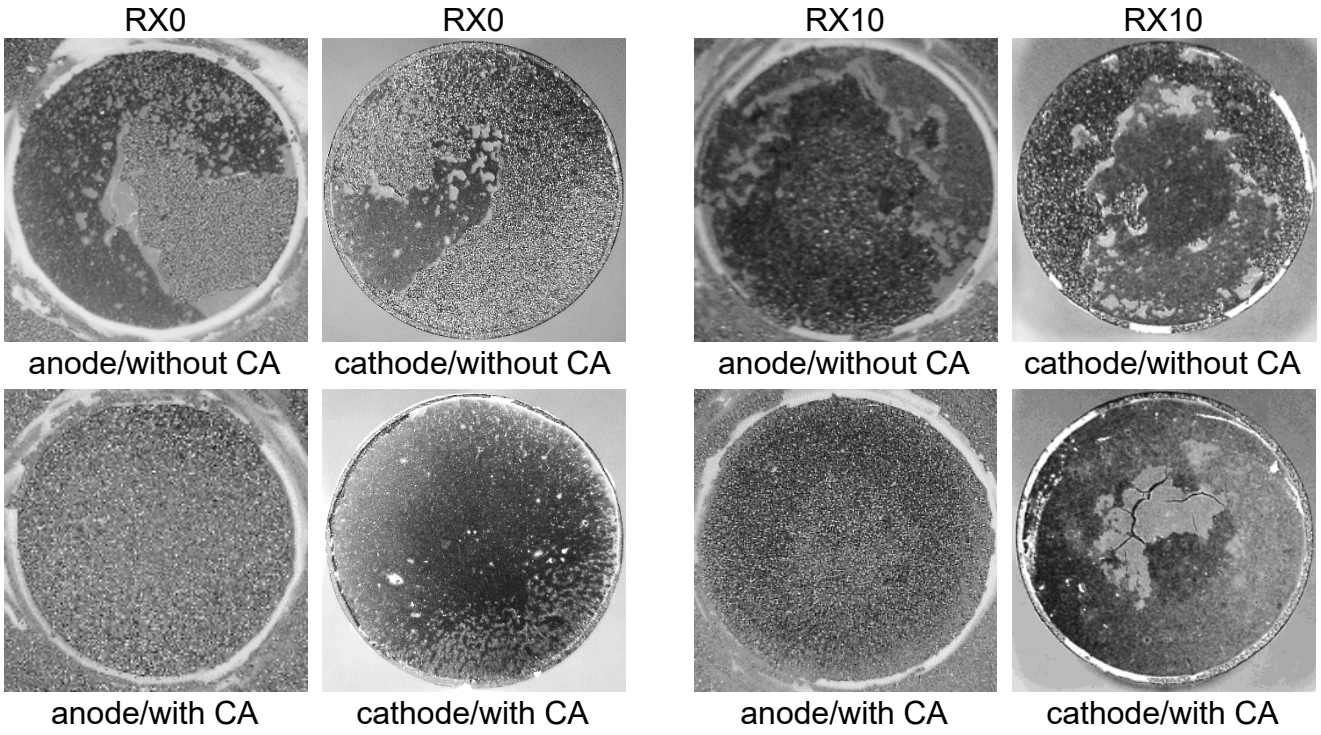

Schematic images of cement residue

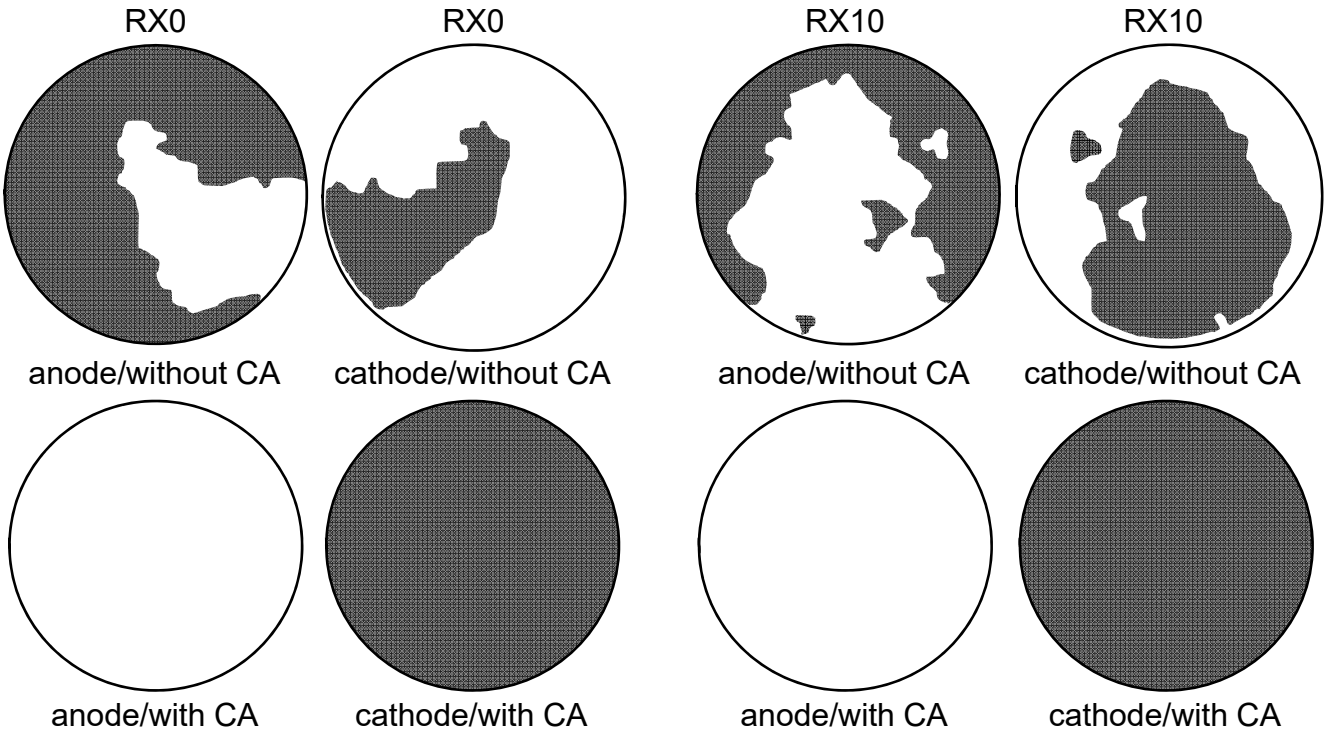

Fig. 8

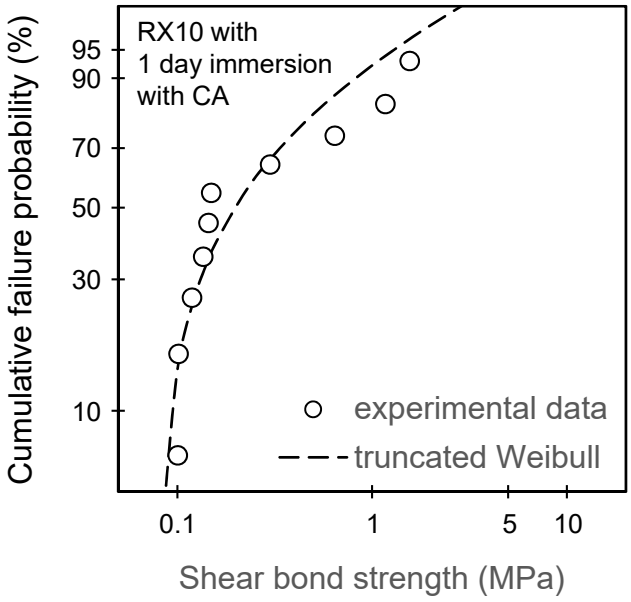
RX10 with
1 day immersion
with CA
95
90
70
50
30
10
Cumulative failure probability (%)
experimental data
truncated Weibull
0.1
1
5
10
Shear bond strength (MPa)

Fig. 9 (100%)